International Journal of GEOMATE, Nov., 2019 Vol.17, Issue 63, pp. 241 - 248
ISSN: 2186-2982 (P), 2186-2990 (O), Japan, DOI: https://doi.org/10.21660/2019.63.98151
Geotechnique, Construction Materials and Environment

GEOELECTRICAL METHODS FOR GEOTHERMAL EXPLORATION IN ENDUT GEOTHERMAL PROSPECT AREA, BANTEN PROVINCE, INDONESIA

*Supriyanto[1], Maryadi Maryadi[1], Dyah Nindita Sahdarani[2] and Ahmad Zarkasyi[3]

[1]Program Studi Geofisika, Fakultas Matematika dan Ilmu Pengetahuan Alam, Universitas Indonesia, Indonesia; [2]Program Studi Geologi, Fakultas Matematika dan Ilmu Pengetahuan Alam, Universitas Indonesia; [3]Center for Mineral, Coal, and Geothermal Resources, Geological Agency, Indonesia

*Corresponding Author, Received: 12 Feb. 2019, Revised: 26 April 2019, Accepted: 15 May 2019

ABSTRACT: Gunung Endut, which is located in Banten Province, Indonesia, holds considerable geothermal energy potential. Besides the existence of the Cikawah (CKW) and Handeuleum (HDL) hot springs, alteration mineral revealed on the surface as a result of contact with heat source are scattered in a relatively wide area to the west of the peak of the volcanic mountain. A geoelectrical method is an essential tool for mapping low resistivity distributions that infers the distribution of mineral alteration. Such an investigation had been conducted in 2006, however, the interpretation of the DC resistivity method was only based on its apparent results which could not precisely image the actual subsurface situation. In this study, we perform audio-magnetotelluric (AMT) technique to obtain resistivity variations at deeper depths. Based on the interpretation results of all the geoelectrical methods, the distribution of impermeable zone with low resistivity is detected in the eastern part of the study area, approximately 3 km to the west of Gunung Endut's peak and 2 km east of the CKW hot spring. The discovery of alteration minerals in these regions supports the interpretation results. The existence of this strong alteration is likely to be controlled by a trending NW-SE fault structure, estimated from the striking analysis and is augmented with both geochemistry analysis and relative gravity study carried out previously. These facts lead to the conclusion that the existence of a geothermal reservoir is estimated between the manifestations of the CKW hot spring and peak of Gunung Endut.

Keywords: Geothermal, Geoelectrical Method, Resistivity, Endut, Indonesia

1. INTRODUCTION

Gunung Endut Geothermal Prospect Area (GPA) has no significant development to date. Despite having the vast potential of geothermal energy as announced by the Geological Agency, further utilization of this 80 MW of thermal energy will not be happening in the near future. One of the problems faced is the clarity of the geothermal system in Endut whether it is dominantly controlled by tectonic activity or by volcanic activity. The signs of the recent Gunung Endut eruption are also less visible on the surface even though the morphology resembles that of a higher mountain than the surrounding area.

Geological Agency Indonesia completed a preliminary survey in 2008 [1]. A follow-up and more detail survey were then conducted by researchers from Universitas Indonesia, including geological, geochemical and geophysical surveys which lasted from 2014 to 2018 [2][3]. Throughout 2018, surface alteration and mineralogy researches were carried out to complete the sparse geological information in Gunung Endut.

Various research in resistivity methods has been performed over the years to gain a deeper and more precise image of a geothermal system [4][5]. The aim of resistivity study is to obtain the information on fluid circulation in the subsurface in the form of subsurface alteration [6]. Altered rocks appear to have lower resistivity values compared to unaltered rocks. The resistivity model can then lead to the determination of the lithologies and permeability properties of the geothermal area [7].

This study is only focused on utilizing the geoelectric method in the Gunung Endut geothermal prospect area to determine resistivity variation with respect to depth. The geoelectric method used is DC-resistivity with Schlumberger configuration to map resistivity variations from surface to shallow depth, and the audio-magnetotelluric (AMT) method to map resistivity variations at deeper depths, as successfully applied in [8][9].

2. GEOLOGICAL CONDITIONS

Gunung Endut GPA is situated in Banten; 70 km SW from Jakarta in the Island of Java, Indonesia. The research area is located within 9261000-9274000 N and 639000-652000 E, Zone 48S in the UTM coordinate. Based on field observation,

Gunung Endut GPA is controlled by the volcanic and tectonic process. Previous geological mapping in 2008 suggested that the research area consist mainly of Quaternary rock (Qpv) lithology originating from the nearest active volcano of Gunung Endut. To the south of Gunung Endut, there are possibilities of Tertiary diorite (Tpg) and granodiorite intrusions [1]. The apparent granodiorite intrusions are elongated upwards to Badui Sedimentary formation consisting mainly of sandstone and limestone. All geological units that exist within the area of interest are shown in Fig. 1.

There are several numbers of hot springs as the surface geothermal manifestations found around the location which are possibly flowing up due to complex subsurface fault systems. These hot springs are situated mainly in the NW direction of Gunung Endut within 6 to 8 km from its highest point as also shown in Fig. 1. As shown in Table 1, the temperature of the hot springs was recorded from 53 - 76 ºC with pH of 6.8 - 7.8 Cl/B ratio obtained from the water analysis from Cikawah (CKW), Handeuleum (HDL) and Gajrug (GJG) revealed that there are two possible reservoirs underneath. These reservoirs have the estimated temperatures of 100 - 127 ºC based on Silica geothermometer.

Table 1. Temperature and other geochemical parameters from each water sample [10].

Spring	Temp (°C)	IB %	pH	Na/K	Cl/B
CKW-1	73	-4.0	6.78	163.8	50
CKW-2	76	-1.0	7.29	33.1	40
HDL	55	1.0	7.59	29.1	31.2
GJG-1	53	1.0	7.65	72.7	83.3
GJG-3	56	-1.0	7.82	48.1	80

Geoindicator calculation of Gunung Endut water chemistry indicates outflow zone surrounding the surface manifestations, as the Na/K ratios are more than 15 [11]. Another detailed geochemical study from the same area and samples had been elaborated in [3].

The study of minerals in altered rock have also been conducted recently. Rock samples were collected and sorted based on the intensity of alteration. Rock samples surrounding the manifestation had a high intensity of alteration [12]. Petrography analysis revealed that the rocks have protolith andesitic composition with several clay minerals as an alteration product. Diffraction analysis confirmed the presence of montmorillonite, kaolinite, and dickite [12].

3. FIELD MEASUREMENTS

Apparent resistivity is a paramount parameter to be analyzed when describing a geothermal system as the components of the system have great contrasts in resistivity value. Resistivity value is affected by physical and chemical properties related to the existing geothermal system such as the salinity of the fluid, alteration, porosity or permeability, and temperature [13]. Ion agitation increases with temperature whereas the viscosity of the fluid decreases, resulting in the lowering of electrical resistivity as the temperature increases [14]. In many cases, high-temperature zones of geothermal reservoirs are located in regions of “anomalously” low value of resistivity. Therefore, the resistivity anomaly is highly useful as an indicator of a geothermal target [6].

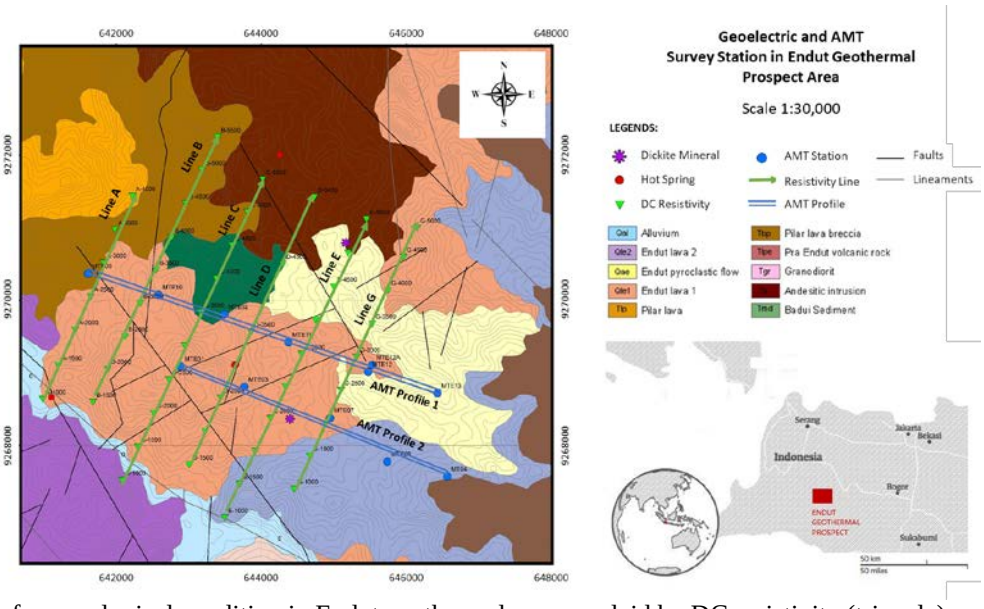

Fig.1 Surface geological condition in Endut geothermal area overlaid by DC resistivity (triangle) and AMT (circle) survey stations and profiles.

There are many mechanisms on the sub-surface that can be responsible for a decreasing of the resistivity value of the surrounding lithology. In the aspect of a geothermal system, where thermal manifestation such as hot spring and fumarole are found, low resistivity can be explicitly caused by the presence of hot water with dissolved minerals in a porous medium. Generally, rocks are poor conductors of electricity and exhibit high resistivity, but when an electrolyte fills the pore spaces, the average resistivity is reduced. Hydrothermally altered rocks that form clay material are better conductors when compared to its protolith. Whenever low resistivity zones are encountered below volcanic active regions, a high-temperature hydrothermal reservoir may be present [15].

In order to get a distinct image of resistivity distribution in both shallow and deep subsurface, two geophysical methods were performed. For the former purpose, an active DC resistivity method was used while the latter was solved by using the audio-magnetotelluric method.

3.1 Resistivity Methods

This exploration technique involves the injection of electric current to the earth and measurement of the potential difference generated afterward. From the information collected, it is then possible to calculate the value of apparent resistivity below the station point by giving the geometrical parameters corresponding to the layout of the survey.

DC resistivity measurement using four-electrodes (referred to as A, B, M, and N) are commonly used in the field. During the acquisition, distances between the current electrodes (A and B) successively increased, while the potential (M and N) electrodes are maintained at a fixed distance from each other and are progressively moved along a line at the surface.

When the distance between the electrodes are enlarged, the depth and volume of subsurface investigated increase and the measurement displays the variation of subsurface resistivity of a certain depth without taking into account the horizontal variation [16]. The apparent electrical resistivity (ρ_a) is then estimated from the measured potential difference,ΔV, as follows,

$$\rho_a = 2\pi\left(\frac{1}{AM} - \frac{1}{BM} - \frac{1}{AN} + \frac{1}{BN}\right)^{-1}\frac{\Delta V}{I} \qquad (1)$$

where AM, BM, AN, and BN are the distance between the respected electrodes, and I am the injected current. This equation is commonly simplified as

$$\rho_a = K\frac{\Delta V}{I} \qquad (2)$$

where K represents the geometrical coefficient that is depending on the survey layout [14].

3.2 Audio-magnetotelluric Exploration

Magnetotellurics (MT) is a passive geophysical method utilizing the time variation of the low-frequency electromagnetic signal that originates from natural sources. The basic principle of MT technique was first introduced in [17][18], and briefly discussed in [19][20]. The MT signal is ranging from 10^{-5} Hz to 10^{4} depending on its origin. This study focuses on the utilization of audio-frequency magnetotelluric (AMT) method instead of the conventional one. AMT method, compared with the common MT, employs the higher frequency parts (above 1 Hz), and therefore has a higher resolution with shallower depth range (up to 1000 m) and more suitable for detailed geothermal field study.

The primary response function derived from AMT survey is the characteristic impedance, Z. This parameter is calculated as the ratio between the orthogonal components of electric (***E***) and magnetic field (***H***). These two site-specific variables are measured using non-polarized electrodes and magnetic sensors (induction coils) respectively. The linear relation between them can be expressed in matrix form as follows,

$$\begin{bmatrix} E_x \\ E_y \end{bmatrix} = \begin{bmatrix} Z_{xx} & Z_{xy} \\ Z_{yx} & Z_{yy} \end{bmatrix}\begin{bmatrix} H_x \\ H_y \end{bmatrix} \qquad (3)$$

where Z_{xx}, Z_{xy}, Z_{yx}, and Z_{yy} are the components of the impedance tensor [21]. Hence, each impedance tensor elements can be written as

$$Z_{ij} = \frac{E_i}{H_j} \qquad (4)$$

where i and j represent the direction of either electric or magnetic field intensity. Thus, the apparent resistivity value is calculated as

$$\rho_a = \frac{|Z_{ij}|^2}{\omega\mu} \qquad (5)$$

where ω is the angular frequency, μ denotes the magnetic permeability [18]. Another analytical parameter in the AMT method is the impedance phase φ, which describes the shift between the orthogonal electric and magnetic field components and is mathematically formulated as

$$\varphi = \tan^{-1}\frac{(imag(Z_{ij}))}{(Real(Z_{ij}))} \quad (6)$$

In homogeneous earth, the phase is always 45° and changes when the fields penetrate into the subsequent layer that has different conductivity [22]. Subsequently, apart from the resistivity, the impedance phase is a useful tool for analyzing the subsurface conductivity structures.

3.3 Survey Design

71 resistivity mapping stations were measured by the Indonesian Geological Agency back in 2006. The aim of this investigation was to map the shallow distribution of resistivity contrast related to the alteration immensely occurred below the surface covering the Gunung Endut GPA

Corresponding to the preliminary geological survey and thermal manifestation found in the location, six resistivity profiles (hereafter referred as Line A, Line B, Line C, Line D, Line E, and Line G) were placed along SW-NE direction. The shortest and longest profile was 3 and 4 km long, respectively. Each of these profiles consisted of 8 to 10 measurement stations with the approximated interval of 500 m. The apparent resistivity from all stations was measured using the Schlumberger array. The current electrodes spacing (AB) is gradually increased from 500 to 2000 m while the potential electrodes are placed in the common center with smaller and fixed separation (MN) of 100 m. With such configuration, it is possible to infer subsurface resistivity up to roughly 500 m in depth.

With the intention to support the previous geoelectrical investigation, as much as 11 AMT sites were placed on two survey lines crossing the DC resistivity profiles (AMT Profile 1 and AMT profile 2) at the center of the prospect area. The average distance between AMT sites is approximately 700 m. This survey is conducted to image the resistivity distribution in NW-SE direction, perpendicular to the available cross-section, to map the alteration as indicated by low resistivity value, and to understand its continuity in the deeper portion.

The AMT data were collected using the tensor equipment, Phoenix MTU-5A systems, along with its designated porous pots (electrodes) and magnetic induction coils. The record length for each data acquisition process is less than 3 hours in average, with the minimum frequency being used is 1 Hz, which could be effectively used to model the subsurface condition slightly more than 1 km, taking into account the penetration depth of AMT signal.

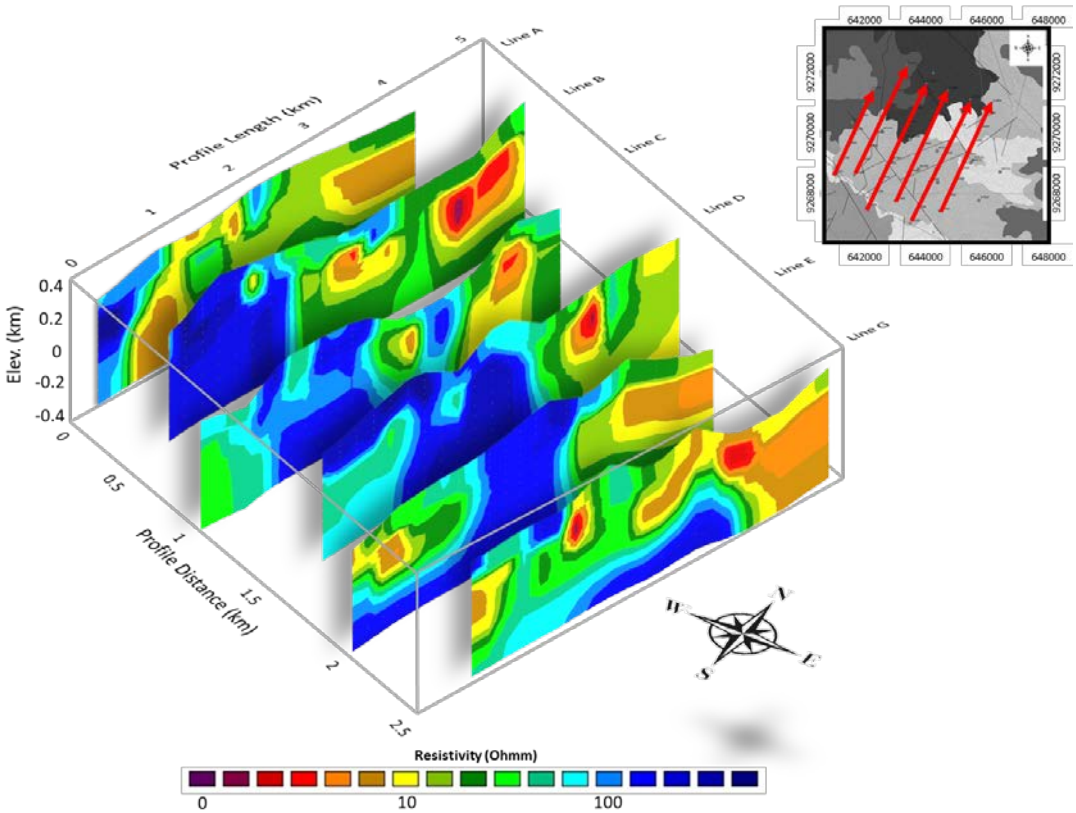

Fig.2 Two-dimensional inversion result of DC resistivity data from all profiles (from upper left to lower right: Line A, Line B, Line C, Line D, Line E, and Line G).

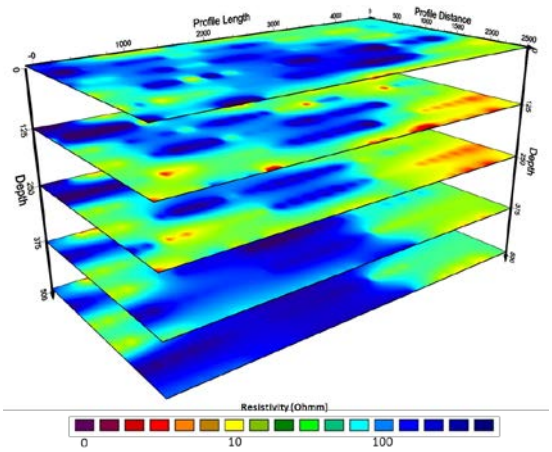

Fig.3 Lateral resistivity mapping under DC Resistivity profiles in 0, 125, 250, 375, and 500 m depth.

4. DATA PROCESSING AND RESULTS

The ultimate objective for both DC resistivity and AMT data processing is to obtain true resistivity map below the surface surrounding the study area from the available data sets. Resistivity contrast plays an important role in delineating a model of the geothermal system, or particularly an anomalous resistive or conductive body in regards to the existing hydrothermal activity. While DC resistivity method can only produce limited model, AMT data, to some extent, can also be applicable to the geostructural study. The integration of DC resistivity and AMT data analysis becomes vital to confirm the final integrated conclusion. In this section, the data processing procedures from each method are separately described.

4.1 DC Resistivity Data Processing

For each resistivity station, there are four resistivity values acquired, in accordance with the variation of the spacing of the current electrodes that describes the average geoelectrical situation in the respected depth. However, the apparent resistivity data could not image the actual state of the subsurface resistivity distribution. In this work, the compiled data from Schlumberger DC resistivity mapping were analyzed based on 2-D inversion to give more reliable information of underground structures according to the resistivity distribution caused by two or three-dimensional complex geological systems in a volcanic area with several different lithologies and fluids circulation. The 2-D inversion scheme implemented in the RES2DINV software is based on the smoothness constrained least-squared method. The result is displayed in both vertical and horizontal cross-section of the resistivity distribution model.

The inversion model result from resistivity profile A, B, C, D, E, and G are plotted together as shown in Fig.2. The horizontal resistivity maps were produced to give a different view for understanding their lateral continuity (or discontinuity). The resistivity value from each depth was extracted and interpolated using inverse distance gridding method. The oblique resistivity maps from five model depth (0, 125, 250, 375, and 500 m) were then accurately stacked as shown in Fig.3.

4.2 AMT Data Analysis

The AMT data time series collected after the acquisition is then processed through several common processing sequences. The time series containing both electric and magnetic field amplitude is regulated with applied filter and manual supervision to control the unwanted noise signal interferences. Fourier Transformation is then utilized to convert the time series into frequency series before finally being calculated and yield the value electrical impedance for each frequency by means of Eq.3.

4.2.1 Strike analysis

The data recorded in the AMT survey are also affected by the subsurface dimensionality and complexity. This concept implies that the information about a subsurface structure such as strike direction could be obtained from the AMT data. Strike direction is where the resistivity value is independent of lateral change. Once the principal axis is determined, the impedance tensor is then rotated in order to increase its two-dimensionality, by minimizing the tensor' diagonal components. The dominant strike direction was estimated using either impedance tensor [23] or phase tensor (PT) [24]. Fig.4 compares the results of the principal strike analysis from both methods for three different frequency level; high, medium, and low.

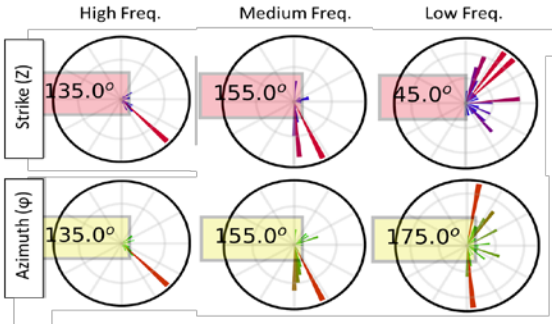

Fig.4 Primary strike direction obtained from impedance tensor (upper part) and phase tensor azimuth (lower part) from three different frequency range. The numbers are CW deviation from the north.

Inferred from Fig.4, both strike angle and PT azimuth shows similar results which indicate the existing fault in the near surface in NW-SE direction. However, the primary strike angle in low-frequency range shows an inconsistency between the values resulting from the impedance and phase tensor analysis. A possible explanation for this might be that there is a more complex structure encountered in the respected depth range.

4.2.2 Two-dimensional inversion model

In order to balance the resolution of resistivity of the cross-section obtained from DC resistivity data, the AMT data inversion was carried out using Occam's 2-D inversion scheme. The idea is to create a smooth resistivity structure by taking the number of the model parameter to be at least the same with the structure encountered in the resistivity profile. As a result, the model would be flexible for any number of significant structure. The possibility of getting an over-parameterized model is controlled by the roughness factor. A detailed explanation is elaborated in [25].

The inversion was implemented to the filtered and rotated data of apparent resistivity and phase from the TE and TM modes. The number of frequency used in the process is 30 ranging from 1 Hz to 10,000 Hz. The inversion process was initialized with a homogeneous half-space model with a resistivity of 50 Ωm, and model depth of 1 km. The model length is the actual AMT profile length added with 0.5 km of additional blocks on both sides. Final inversion results from two AMT profiles are shown in Fig. 5. The model RMS misfits obtained after 20 iteration processes are 8.7 and 5.5 for AMT Profile 1 and AMT Profile 2, respectively.

5. DISCUSSIONS

With respect to the results from DC resistivity survey shown in Fig.2 and Fig.3, it appears that the southern part of the study area is dominated by high resistivity, while less than a half portion in the northern part is indicated a minor appearance of low resistivity anomalies. These results are consistent with the model produced from the AMT method. The combined resistivity model from both techniques is shown in Fig.6.

One noticeable inconsistency occurs in the central region of the research area, where there is a quite significant amount of high conductivity anomaly appeared in the AMT model is undetected in the other. This discrepancy is perhaps related to the inability of DC resistivity method or, in particular, Schlumberger array to interpret a complex horizontally layered structure and lateral variation (when the station spacing is way too wide). Another possible explanation of this could also be a high disruption in AMT responses due to artificial noise, which is a definite disadvantage of a passive electromagnetic method like AMT, as the particular sites are located near an urban area. However, this difference does not really affect the overall interpretation.

Based on the resistivity contrast from geoelectric and AMT inverted model and strike analysis of AMT Data, there is a possibility of an existing fault in the center of survey area next to CKW hot springs (Fig. 6) which is unseen in the current geological structure map (Fig.1). This fault system is expected to be responsible for the hydrothermal fluid pathway to the surface which then appears as the hot spring manifestation. From the geochemistry study, a significant number of kaolinite and other related minerals are found in the vicinity of this deduced fault, meaning that the specific area could have been passed by the fluids. These findings are also consistent with the gravity study carried out previously.

On the other hand, a massive resistive body found between HDL and CKW indicates that both hot springs originated from different reservoir system. This finding also accords with the earlier discovery resulting from the water sample analysis (explained in Section 2), which shows a similar conclusion.

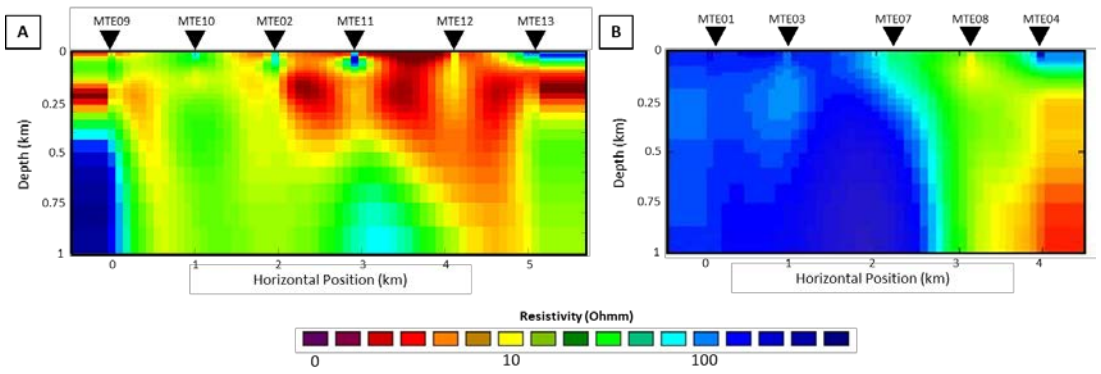

Fig.5 Two-dimensional resistivity distribution model from (A) AMT Profile 1 and (B) AMT Profile 2 resulted from AMT inversion using Occam's 2-D inversion.

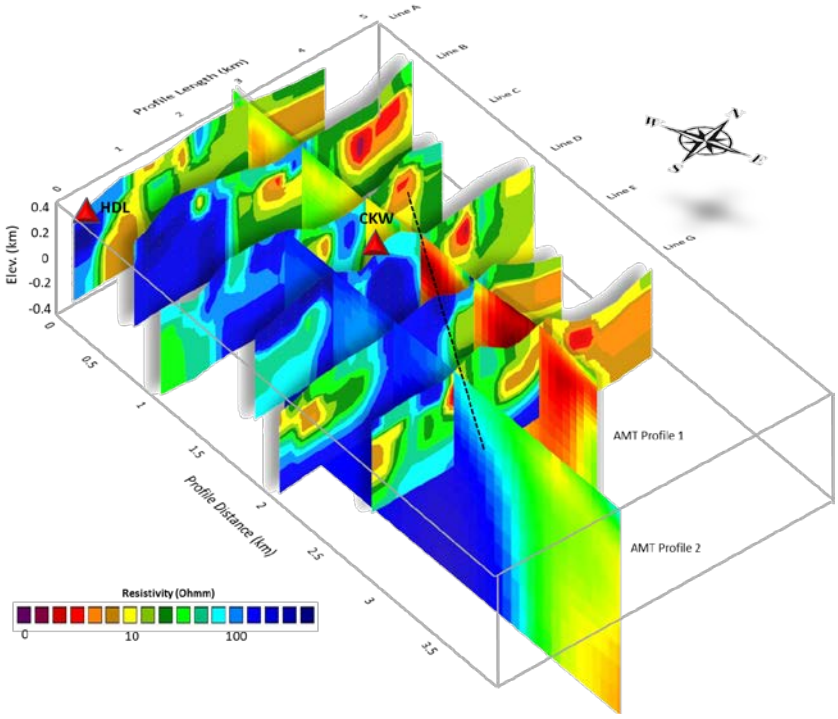

Fig.6 Combined image of the resistivity distribution model from DC resistivity and AMT investigation in the prospect area. The springs are indicated by triangles. A predicted fault system is represented by a dashed line.

There is no evidence of a conductive impermeable layer found beneath the surface in the center of the survey area, which is also indicated that no geothermal reservoir exists below the exact location. The indication of that interesting feature is occurred in the east direction at about 3 km west from Gunung Endut's summit, and 2 km east of the CKW hot spring. This result again matches those observed in geochemistry study, which stated that the manifestations appear in the surrounding are possibly come by means of the outflow mechanism.

Since the location of the reservoir is still could not be detected, it is suggested to conduct a magnetotelluric prospection in about the eastern and south-eastern part of the current study area. This recommendation is based on a slight appearance of a highly conductive anomaly found in the east flank of the AMT profiles which hypothetically spread and enlarged towards the SE direction. By continuing a more extensive study in the region, the geothermal system and potential reserved beneath the Gunung Endut Prospect Area could be more accurately understandable, in order to advance to the development stage

6. CONCLUSION

The subsurface resistivity investigation using DC resistivity method and audio-frequency magnetotelluric survey yields a good result. Despite some slight differences, the resistivity model derived from both ways share similar outcomes and findings. The geochemical analysis could really help to understand and support the result as the resistivity value is closely related to the geochemical parameter and activity.

There are some interesting findings that need to be underlined. Firstly, a massive resistive body separates the HDL and CKW springs which suggests that both manifestations are coming from two different reservoirs. Secondly, a possibility an existing fault connected to CKW hot spring that is delineated from the resistivity contrast, strike analysis and supported by rock minerals study. Finally, the conductive layer anomaly indicated in the eastern part and not in the center part of the research area. This finding leads to the conclusion that the existence of a geothermal reservoir is estimated between the manifestations of the CKW hot spring and the peak of Gunung Endut. An advanced study in this specific location is highly suggested for a more extensive interpretation.

7. ACKNOWLEDGMENTS

We acknowledge the Ministry of Energy and Mineral Resources of Indonesia for making the geoelectrical data available for this study, and the Ministry of Research, Technology and Higher Education of Indonesia for financial support through the scheme of Hibah PDUPT with the contract number: 383/UN2.R3.1/HKP05.00/2018.

8. REFERENCES

[1] Widodo S., Kusnadi D., Kholid M., and Rezki Y., Evaluasi Potensi Panas Bumi Daerah Gunung Endut, Kabupaten Lebak, Provinsi Banten (In Bahasa), in Prosiding Hasil Kegiatan Lapangan Pusat Sumber Daya Geologi, 2009.

[2] Supriyanto, Noor T., and Suhanto E., Analysis Of Gravity Data Beneath Endut Geothermal Prospect Using Horizontal Gradient And Euler Deconvolution, in AIP Conference Proceedings, 2017.

[3] Supriyanto, Rokhmatuloh, Sobirin R., and Suhanto E., The Effect of Gravity Measurement Distribution Points On Interpretation Of Gravity Data In The Gunung Endut Geothermal Prospect Area, Indonesia, Int. J. of GEOMATE, Vol. 14, No. 41, 2018, pp. 60–67.

[4] Bromley C. J., and Española O. S., Resistivity Methods Applied To Geothermal Exploration In The Philippines, in Pacific Geothermal Conference, 1982, pp. 447–452.

[5] Arnason K., Karlsdottir R., Eysteinsson H., Flovenz O. G., and Gudlaugsson S. T., The Resistivity Structure Of High-Temperature Geothermal Systems In Iceland, in Proceedings of the World Geothermal Congress, 2000, pp. 923–928.

[6] Ussher G., Harvey C., Johnstone R., and Anderson E., Understanding The Resistivities Observed In Geothermal Systems, in World Geothermal Congress 2000, 2000, No. May, pp. 1915–1920.

[7] Anderson E., Crosby D., Ussher G., and Zealand N., Bulls Eye! - Simple Resistivity Imaging To Reliably Locate The Geothermal Reservoir, in World Geothermal Congress 2000, 2000, pp. 909–914.

[8] Barcelona H., Favetto A., Peri V. G., Pomposiello C., and Ungarelli C., The Potential Of Audiomagnetotellurics In The Study Of Geothermal Fields: A Case Study From The Northern Segment Of The La Candelaria Range, Northwestern Argentina, J. Appl. Geophys., 2013.

[9] Monteiro Santos F. A., Andrade Afonso A. R., and Dupis A., 2D Joint Inversion Of Dc And Scalar Audio-Magnetotelluric Data In The Evaluation Of Low Enthalpy Geothermal Fields, J. Geophys. Eng., 2007.

[10] Risman C., Sahdarani D. N., Sihombing F. M. H., and Supriyanto, Geochemical Fluids Assessment Of Gunung Endut Geothermal Area, Banten Province, Indonesia, in The International Conference on Geoscience, 2018.

[11] Nicholson K., Contrasting Mineralogical-Geochemical Signatures Of Manganese Oxides; Guides To Metallogenesis, Econ. Geol., Vol. 87, No. 5, 1992, pp. 1253–1264.

[12] Primayudha F., The Distribution Of Hydrothermal Clay Using Difraction Method And Petrography Analysis In Gunung Endut, Banten, Universitas Indonesia, 2018.

[13] Hersir G. P., and Árnason K., Resistivity of Rocks, in Short, Course IV on Exploration for Geothermal Resources, UNU-GTP , KenGen and GDC, Kenya, 2009.

[14] Samouëlian A. *et al.*, Electrical Resistivity Survey In Soil Science : A Review . To Cite This Version : HAL Id : Hal-00023493, 2006.

[15] DiPippo R., Geothermal Power Plants, Vol. 7. 2012.

[16] Loke M. H., Constrained Time-Lapse Resistivity Imaging Inversion, in Symposium on the Application of Geophysics to Engineering and Environmental Problems 2001, 2001.

[17] Tikhonov A. N., On Determining Electric Characteristics Of The Deep Layers Of The Earth's Crust, Dolk. Acad. Nauk. SSSR, Vol. 73, 1950, pp. 295–297.

[18] Cagniard L., Basic Theory of The Magneto - Telluric Method of Geophysical Prospecting, Geophysics, Vol. 18, No. 3, 1953, pp. 605–635.

[19] Berdichevsky M. N., and Dmitriev V. I., Models And Methods Of Magnetotellurics. 2008.

[20] Simpson F., and Bahr K., Practical Magnetotellurics. 2005.

[21] Vozoff K., The Magnetotelluric Method, in Electromagnetic Methods in Applied Geophysics: Volume 2, Application, Parts A and B, M. N. Nabighian, Ed. Society of Exploration Geophysicists, 1991, p. 991.

[22] Naidu G. D., Deep Crustal Structure Of The Son-Narmada-Tapti Lineament, Central India, 2012, pp. 13–36.

[23] Swift C. M., A Magnetotelluric Investigation Of An Electrical Conductivity Anomaly In The Southwestern United States, Magnetotelluric methods, Vol. Ph.D., 1967, p. 211.

[24] Caldwell T. G., Bibby H. M., and Brown C., The Magnetotelluric Phase Tensor, Geophys. J. Int., Vol. 158, No. 2, 2004, pp. 457–469.

[25] De Groot-Hedlin C., and Constable S., Inversion Of Magnetotelluric Data For 2D Structure With Sharp Resistivity Contrasts, Geophysics, Vol. 69, No. 1, 2004, pp. 78–86.